Chain Folding in EBEE Semicrystalline Diblock Copolymers

Konstadinos C. Douzinas and Robert E. Cohen*

Department of Chemical Engineering, Massachusetts Institute of Technology, 77 Massachusetts Avenue, Cambridge, Massachusetts 02139-4307

Received February 27, 1992; Revised Manuscript Received May 15, 1992

ABSTRACT: X-ray pole-figure analysis and small-angle X-ray scattering were used to determine the lattice unit cell orientation with respect to the lamellar microstructure for semicrystalline diblock copolymers of ethylene-*co*-butylene-*b*-ethylethylene (EBEE). The X-ray data indicate that the orientation of the crystallized EB chains is perpendicular to the lamellar normals, unlike the chain folding which has been observed in semicrystalline homopolymers and proposed for semicrystalline diblock copolymers where the crystallized chains align roughly parallel to the lamellar normals. The unusual chain folding observed for EBEE is attributed to the influence of topological constraints on the EB blocks which crystallize within the amorphous lamellar microdomains present in the heterogeneous melt phase of the block copolymers.

Introduction

In a previous paper[1] we used small-angle X-ray scattering to test the two scaling laws[2,3] which have been proposed to describe the molecular weight dependence of the lamellar domain spacing of semicrystalline diblock copolymers. We found that both theories did an adequate job of describing the general form of the molecular weight dependence of the lamellar long period, D, which can be written in the form

$$D \propto Z_t Z_a^{-n} \tag{1}$$

where Z_t is the total degree of polymerization of the semicrystalline diblock copolymer and Z_a is the degree of polymerization of the amorphous block. The best fit value[1] for the exponent n agreed closely with the prediction of $^5/_{12}$ given by one of the models.[2]

The question of chain organization within the ordered structure of heterogeneous block copolymers in bulk has been addressed extensively in the past for the case of wholly amorphous block copolymers;[4-15] the block sequences behave essentially as Gaussian coils, although some measurable anisotropic distortions have been documented.[11,15-17] For the case of semicrystalline block copolymers, less information exists in regard to the spatial organization of the block sequences; it has been presumed[2,3,18] that random coils exist in the amorphous domains and that conventional chain folding (i.e., chains parallel to[19,20] or perhaps slightly inclined[11,21] with respect to the lamellar normals) takes place in the crystalline domains. The limited amount of available information[22,23] on chain folding in semicrystalline block copolymers appears to support this presumption, although the evidence has been obtained for the case in which direct crystallization from a homogeneous melt or solution was the mechanism controlling the formation of the final morphology; in such cases where crystallization precedes microphase separation, conventional chain folding is expected to occur. However, previous work in our laboratory[24,25] has shown clearly that routine processing methods from solution or the melt will often lead to the occurrence of amorphous microphase separation prior to the crystallization of semicrystalline block copolymers. In this case, when chain folding occurs, it must take place within the confines of the already-ordered, heterogeneous morphology; in the work presented below we will demonstrate that this latter situation causes the chains of the crystallizable block of the copolymer to fold in such a way that the chain direction is essentially perpendicular to the lamellar normals, i.e., 90° away from the direction expected for conventional chain-folded materials.

Table I
Molecular Weight Characterization of Poly(EBEE) Samples

sample	$M \times 10^{-3}$	sample	$M \times 10^{-3}$
EBEE-1	60/7	EBEE-142	52/89
EBEE-2	36/6	EBEE-144	62/72
EBEE-136	82/76	EBEE-146	91/71
EBEE-137	78/40	EBEE-148	124/63
EBEE-138	35/53	EBEE-150	62/102
EBEE-140	81/35		

Experimental Section

Semicrystalline poly(EBEE) diblock copolymer samples[1] were prepared by catalytic hydrogenation of precursor amorphous diblocks of 1,4-polybutadiene-*b*-1,2-polybutadiene, poly(4B2B), which were polymerized anionically from 1,3-butadiene. The 1,4 blocks contained 45% cis-1,4, 45% trans-1,4, and 10% vinyl repeat units. The 1,2-PB blocks were 99% atactic 1,2. The homogeneous catalytic hydrogenation procedure has been described in detail elsewhere.[1,24,26] The hydrogenation reaction goes to completion, and there is no degradation, chain scission, or chain coupling. The molecular weights of the poly(4B2B) precursor diblocks were measured using GPC complemented by H^1 NMR, and the corresponding molecular weights of poly(EBEE) were calculated using the stoichiometry of the hydrogenation reaction. Table I contains molecular weight characteristics of the poly(EBEE) samples used in this study.

Poly(EBEE) films were prepared by spin casting[27] from 5 wt % xylene solutions at 95 °C, which is close to the melting point for the EB block of the copolymers.[28] The films were subsequently dried under vacuum. This processing history leads to microphase separation prior to crystallization.[1,24] The long-range orientation of the lamellae in these samples was improved by applying oscillating rotational shear or uniaxial compression on the cast films[28] at temperatures above the melting point of the EB block.

The morphology of the poly(EBEE) samples was determined from SAXS analysis at room temperature, using a Rigaku rotating-anode Cu Kα X-ray source operating at 40 kV and 30 mA, with a Charles Supper double-mirror-focusing system and a Siemens–Nicolet 2D area detector with a resolution of 200 μm. The sample-to-detector distance was 260 cm, and background scattering was reduced by a helium-filled beamline tube.

The form and dimensions of the lattice unit cell and its orientation with respect to the lamellar superstructure, for both the as-cast and the oriented poly(EBEE) samples, were determined by wide-angle X-ray diffraction (XRD) and pole-figure (PFG) analysis, respectively. A Rigaku RU-200BH high-brilliancy X-ray generator operating at 50 kV and 60 mA was used. The geometry used for XRD and PFG analysis is shown in Figure 1.[29] The sample was placed on a rotating holder that

0024-9297/92/2225-5030$03.00/0

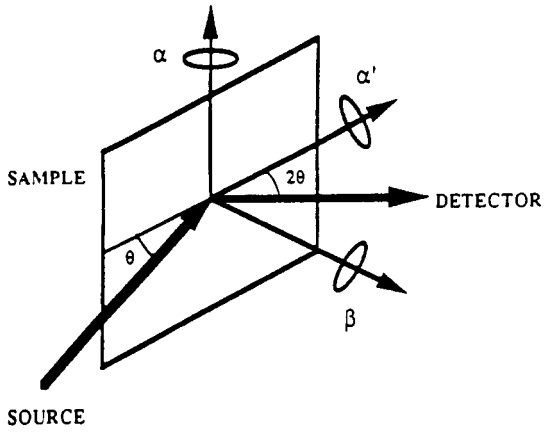

Figure 1. Pole-figure analysis geometry.

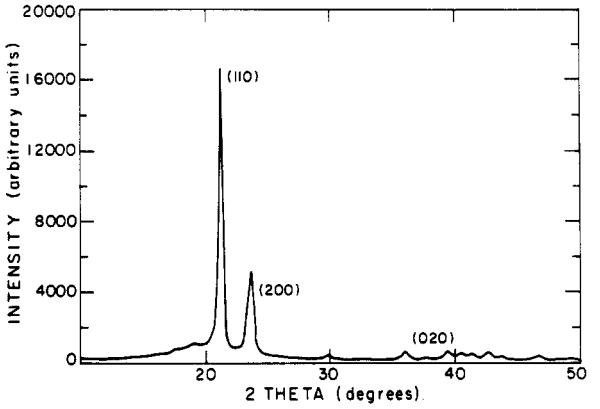

Figure 2. 2θ scan for a HDPE homopolymer.

allowed variation of take-off angles α and α', the rotation angle β, and the Bragg angle θ. A Soller slit box with a nickel filter and receiving a Schulz slits was used to isolate Cu Kα radiation and to control the divergence of the diffraction beam. All experimental parameters were controlled by a Microvax computer running DMAX-B software.

Results

A. Crystalline Nature of Poly(EBEE). For comparison with our copolymers, a 2θ scan for a standard sample of a high-density polyethylene (HDPE) homopolymer is shown in Figure 2. Several diffraction peaks are observed corresponding to the (110), (200), and (020) diffraction planes of the orthorhombic unit cell of polyethylene.[30] Howard and Crist[31] have studied the unit cell of EB random copolymers with varying butylene content, and they have shown that such polymers, which correspond to our EB block, also crystallize in the body-centered orthorhombic system. They found, however, a slight enlargement of the lateral (i.e., a- and b-axes) unit cell dimensions, apparently due to some accommodation of the ethyl side chains by the crystal lattice.[31] A typical 2θ scan for a poly(EBEE) block copolymer sample is shown in Figure 3. In addition to the diffraction peaks for the (110), (200), and (020) planes, a broad amorphous halo centered around $2\theta = 20°$ is observed. The intensity of the amorphous halo increases as the amorphous block content of the poly(EBEE) sample increases. The EB blocks of poly(EBEE) crystallize in the same orthorhombic lattice system as the HDPE homopolymer and the EB random copolymer. A schematic of the unit cell for the body-centered orthorhombic system with the major diffraction planes is shown in Figure 4 where the crystallized polymer chains are parallel to the c-axis of the unit cell.

From the positions of the peaks in the 2θ scans of the poly(EBEE) samples it is possible to calculate the a- and

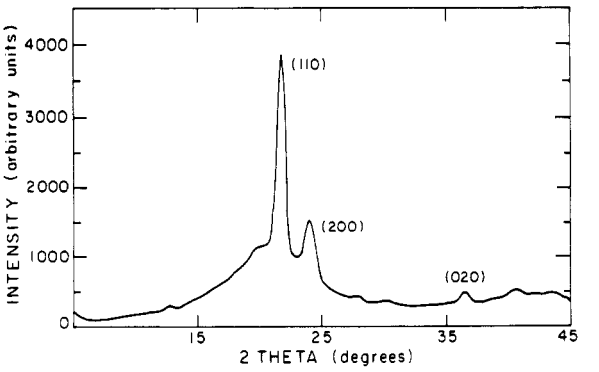

Figure 3. 2θ scan for poly(EBEE)-1.

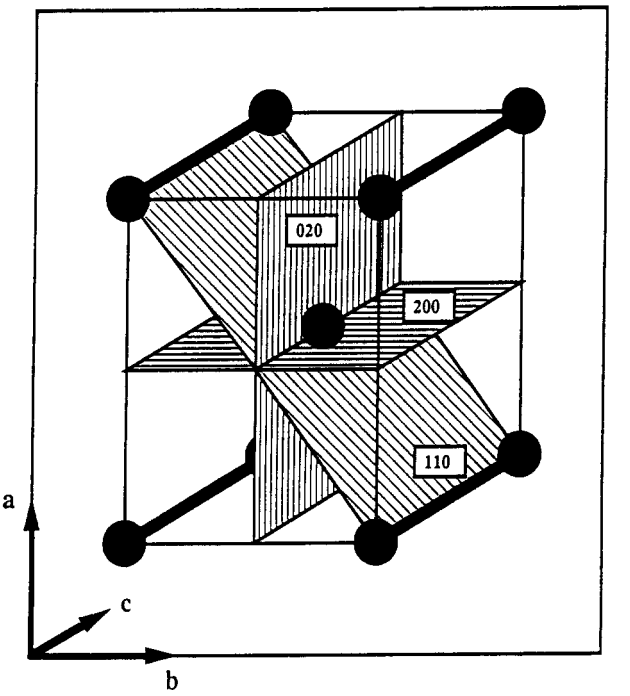

Figure 4. Unit cell for the body-centered orthorhombic system.

Table II
Unit-Cell Dimensions for Poly(EBEE) Diblock Samples

sample	$D(110)$	$D(200)$	a-axis (Å)	b-axis (Å)	Z_s/Z_t
EBEE-1	4.188	3.799	7.60	5.02	0.108
EBEE-2	4.055	3.675	7.35	4.86	0.146
EBEE-136	4.237	3.799	7.60	5.10	0.480
EBEE-137	4.168	3.743	7.49	5.02	0.398
EBEE-138	4.237	3.831	7.66	5.09	0.600
EBEE-140	4.217	3.791	7.58	5.07	0.304
EBEE-142	4.158	3.743	7.49	5.00	0.632
EBEE-144	4.207	3.799	7.60	5.05	0.535
EBEE-146	4.120	3.736	7.47	4.94	0.436
EBEE-148	4.298	3.864	7.73	5.17	0.337
EBEE-150	4.227	3.831	7.66	5.07	0.620
EB-18[a]	4.146	3.760	7.52	4.97	0
EB-39[a]	4.154	3.765	7.53	4.98	0
HDPE[b]	4.110	3.705	7.41	4.94	0

[a] EB-18 has 18 ethyl side chains per 1000 · atoms, and EB-39 has 39 ethyl side chains per 1000 C atoms (from Howard and Crist). [b] From Spruiell and Clark.[30]

b-axis dimensions of the orthorhombic unit cell using the relationship[30]

$$1/d_{hkl}^2 = h^2/a^2 + k^2/b^2 + l^2/c^2 \quad (1)$$

where d_{hkl} is the spacing between planes with indices h, k, and l and a, b, and c are the dimensions of the unit cell. The values obtained are presented in Table II. It is clear that the unit cell of poly(EBEE) is very slightly larger than that of the HDPE homopolymer and the EB random

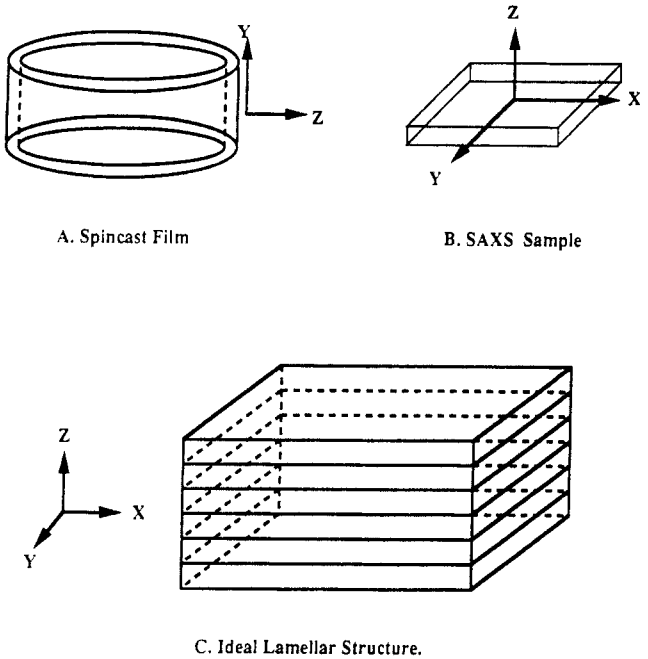

Figure 5. Sample orientation for SAXS analysis.

copolymer, and there is no significant trend with amorphous content or copolymer molecular weight.

Thermal analysis of poly(EBEE) samples confirmed previous findings[31] of a melting point depression for EB copolymers in comparison to HDPE and LDPE homopolymers. For poly(EBEE) samples the melting point temperature ranged from 95 to 105 °C. These values are consistent with those observed for EB copolymers with similar side-chain content.

B. Lamellar Morphology of Poly(EBEE). SAXS measurements were performed on the full series of poly(EBEE) samples (Table I) to determine the nature and spacing of the morphology. Each sample was irradiated parallel to the X, Y, and Z directions as shown in Figure 5 and discussed in detail elsewhere.[1] Arcs were observed on the 2D SAXS detector when the samples were irradiated parallel to the X and Y directions, and there was no significant scattering when the samples were irradiated parallel to the Z direction. Thus the poly(EBEE) samples all display a lamellar morphology with the lamellae predominantly parallel to the XY plane (Figure 5). The fact that arcs were observed, instead of spots, indicates that the lamellar orientation is not perfect and that there exists a degree of lamellar misorientation and/or waviness. Figure 6 presents quantitative information on the degree of perfection of the lamellar orientation in the EBEE-146 copolymer, both as-cast from xylene at 95 °C and after uniaxial compression at 125 °C to a compression ratio (initial height/final height) of 6.7. It is clear that considerable improvement in the prefection of the lamellar orientation was achieved using the compressive deformation. Similar but not as extensive improvement in lamellar orientation was achieved using oscillating shear.[28]

The fact that the poly(EBEE) samples are heterogeneous in the melt and that the order–disorder transition precedes crystallization during preparation of poly(EBEE) samples by spin casting was confirmed using high-temperature SAXS measurements and dynamic mechanical spectroscopy analysis.[28] At temperatures above the melting point of EB, a distinct SAXS peak is observed near $Q = 0.012$ (where $Q = 4\pi\lambda^{-1} \sin\theta$, λ is the wavelength, 1.54 Å, of the X-rays, and θ is half of the scattering angle), indicating a heterogeneous morophology for the amorphous poly(EBEE)-137 diblock. The intensity of the peak

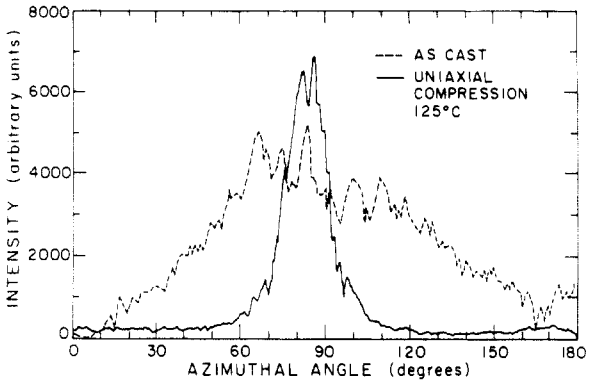

Figure 6. Intensity as a function of azimuthal angle at the SAXS maximum for poly(EBEE)-146 specimens as-cast from xylene at 95 °C and after further orientation by uniaxial compression. Perfectly oriented lamellae in the XY plane would result in a sharp spike at 90°.

decreases with increasing temperature, but the peak clearly persists up to 214 °C, which was the highest temperature employed. This indicates that poly(EBEE)-137 is heterogeneous in the melt at least up to 214 °C. SAXS measurements obtained upon cooling showed a very slight trend toward higher Q (smaller lamellar spacing) as the temperature dropped through the melting point; within the precision of the data[28] a more detailed analysis was not warranted. Previous investigators have also shown that for heterogeneous block copolymers in the melt, log–log plots of loss modulus G'' versus storage modulus G' vary with temperature up to a certain critical value and then become temperature independent[32] with a slope 2 for samples in the homogeneous disordered state. In the case of poly(EBEE)-137 the slope of the log G' vs log G'' curve varied up to the highest measured temperature of 250 °C at which point a slope of 2 was not yet achieved. This plot also suggests that poly(EBEE)-137 is heterogeneous in the melt. Similar rheological and SAXS experiments and some qualitative observations of shape changes[34] for macroscopic chunks of the various copolymers indicated that all of the samples listed in Table I are heterogeneous in the melt, with a few samples first showing some tendency toward homogenization in the temperature range of 140–170 °C.[28]

C. Chain-Folding Behavior of Poly(EBEE). Pole-figure analysis was performed on poly(EBEE) samples to determine the orientation of the orthorhombic unit cell with respect to the lamellar morphology. The application of pole-figure analysis as a mapping tool for the determination of crystallite orientation in the solid state has been described in the literature.[29,35–37] Pole figures for the (200) and (020) planes of poly(EBEE)-137 are shown in Figures 7–9. These pole figures are shown in the form of normalized contour plots where the nominal value of 10 represents the highest intensity of plane normals. In all cases there is a single distinct concentration of (200) poles coming out of the plane of the figure, i.e., nearly parallel to the Z-axis of the sample. This indicates clearly that the normal to the a-plane of the unit cell, i.e., the a-axis, is parallel to the Z-axis (see Figure 5) of the sample. For the (020) or b-plane of the unit cell, the regions of high intensity are distributed around the circumference of the pole figure. This signifies that the normal to the b-plane, i.e., the b-axis of the unit cell, is normal to the Z-axis of the sample, i.e., parallel to the XY-plane of the sample, but its direction is not well-oriented within the XY-plane. Pole figures for as-cast and oriented poly(EBEE)-146[28] showed exactly the same features: a concentration of (200) poles in the Z-direction and (020) pole density distributed

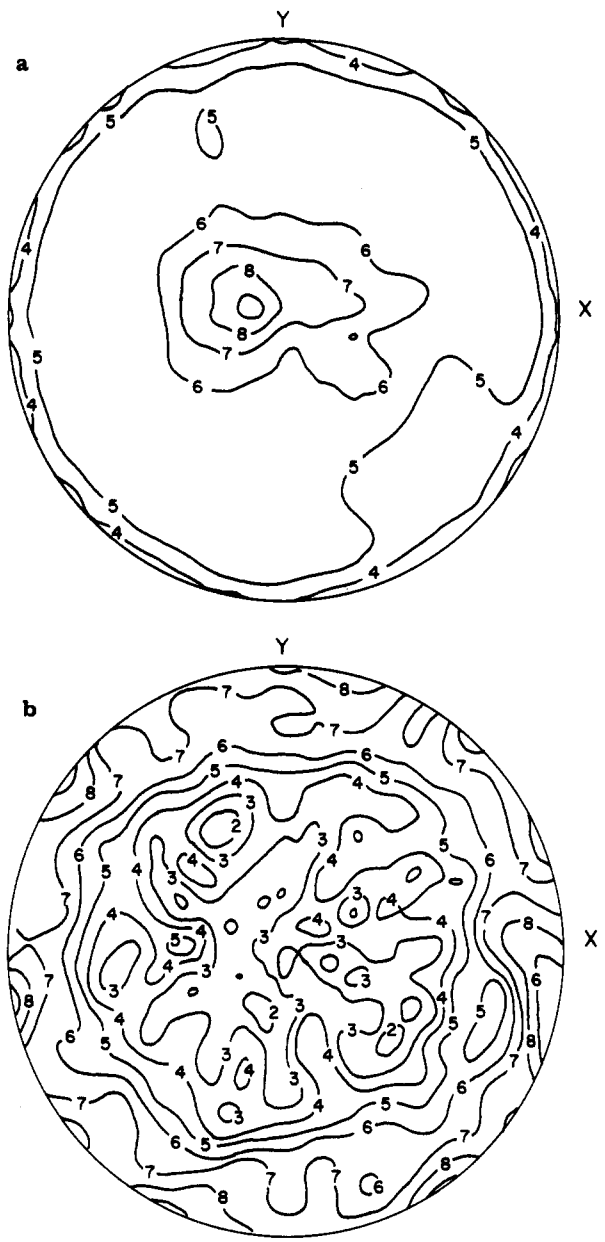

Figure 7. Pole figures of poly(EBEE)-137 as cast at 95 °C: (a) (200) plane normals; (b) (020) plane normals.

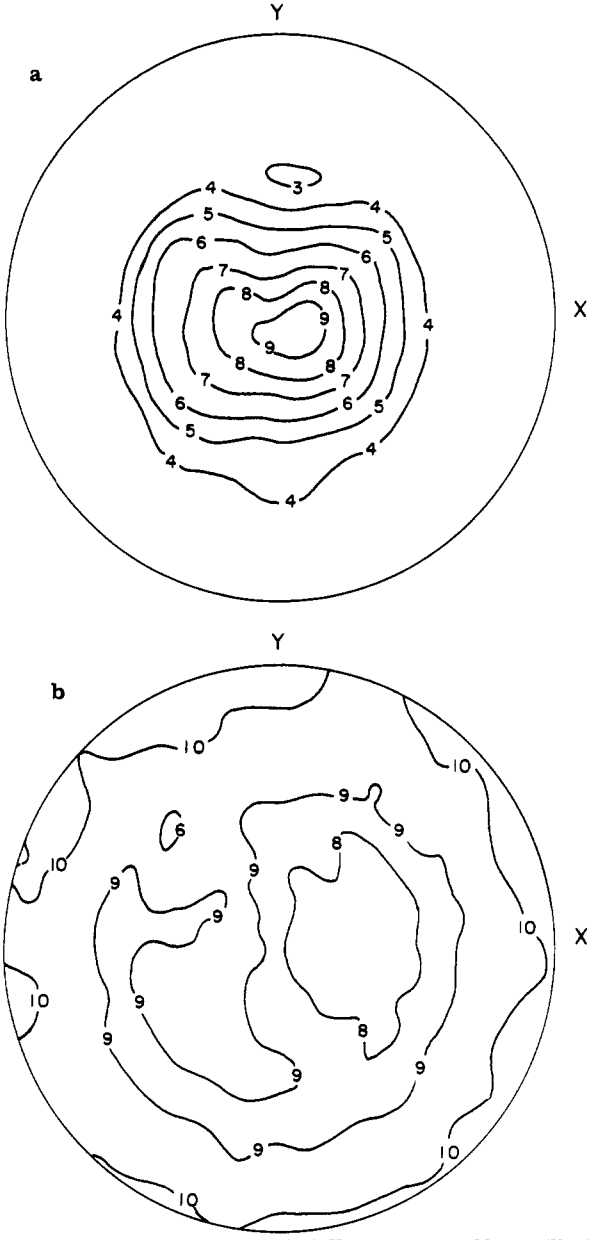

Figure 8. Pole figures of poly(EBEE)-137 oriented by oscillating rotational shear at 115 °C: (a) (200); (b) (020).

around the pole figure circumference, normal to Z. Thus, the orientation of the unit cell in the EBEE-146 specimens is the same as the orientation of the unit cell in poly(EBEE)-137. This unit cell orientation is shown schematically in Figure 10.

Discussion

The experimental evidence presented in the preceding sections indicates clearly that the crystallized EB chains of poly(EBEE) are predominantly parallel to the plane of the lamellar superstructure and therefore fold in some manner similar to that shown schematically in Figure 11. To explain this unorthodox behavior, it is necessary to take into account the processing history of our samples and the interaction of the two major ordering mechanisms: crystallization and order–disorder transition. We have found[1,24,25,28] that morphologies controlled by crystallization are entirely different from morphologies controlled by the order–disorder transition.

In cases where crystallization occurs from a homogeneous melt or solution preceding the microphage separation, kinetics control the final morphology and the crystallizable chains can follow the classical nucleation and growth process.[38] This leads to conventional chain-folding behavior with the folds at the lamellar surfaces and the chains roughly normal to these surfaces. For semicrystalline diblock copolymers, on the other hand, it is possible to obtain samples in which crystallization occurs in a heterogeneous melt or solution. In such cases, the crystallizable chains find themselves in the form of topologically restricted coils located within microdomains, within which they must crystallize. Depending on the type of microdomain, the chains may be geometrically restricted in three (spheres), two (cylinders), or one (lamellae) dimension. For the case of lamellae this evidently can lead to the unexpected chain folding (chains essentially parallel to the interfaces between the block copolymer domains) which we have observed; the folds are therefore embedded within the semicrystalline lamellae as suggested in Figure 11.

Because we have seen no evidence of a repeating long period perpendicular to the lamellar normals, it is probable that the chain folds are spaced at irregular intervals along each EB chain as suggested in Figure 11. Since our EB blocks have 2–3 ethyl side branches per 100 carbon atoms,

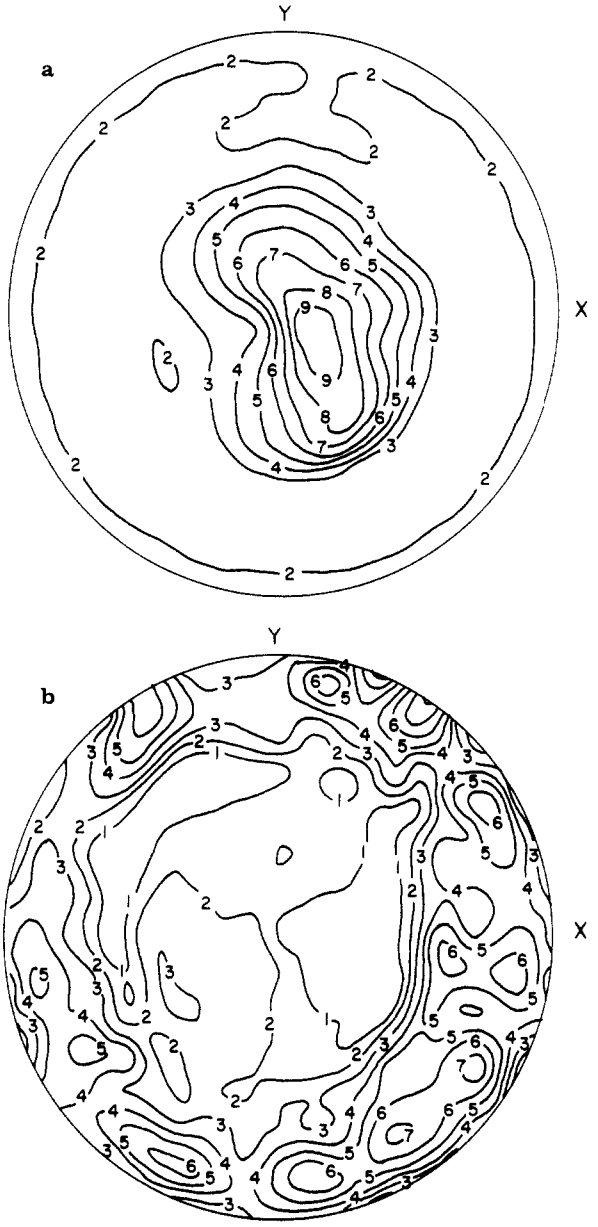

Figure 9. Pole figures of poly(EBEE)-137 oriented by oscillatory rotational shear at 90 °C: (a) (200); (b) (020).

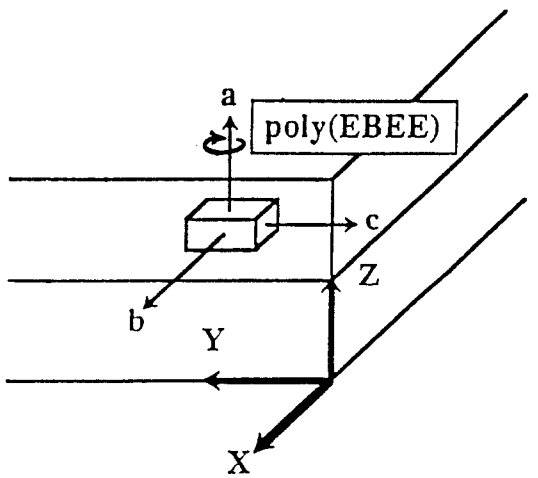

Figure 10. Unit-cell orientation with respect to the lamellar superstructure.

and these branches appear at irregular intervals along the EB chain, it is possible that there is an association between folds and side chains. Although folding can occur at locations without side chains, it is reasonable to expect

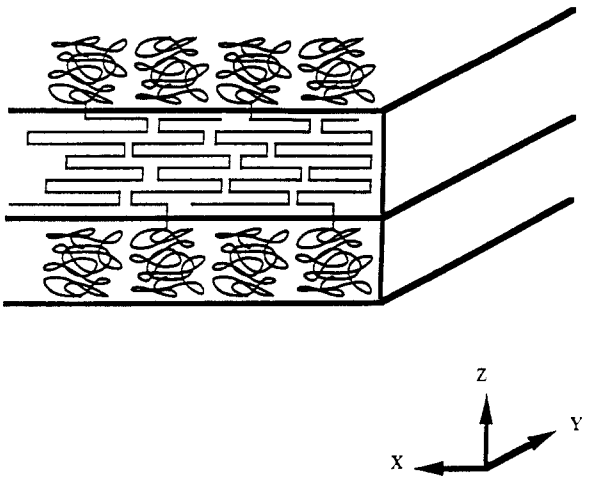

Figure 11. Proposed chain-folding model for EBEE block copolymers.

that most of the side chains must be largely excluded by the crystallized chains; therefore, the unusual "sideways" chain folding, revealed clearly by the data we have obtained for the EBEE diblock copolymers, might arise *because* of the need to accommodate the EB side chains. While we cannot entirely dismiss this argument, we do note that conventional chain folding occurs in ordinary EB polymers (not block copolymers) with similar side-chain contents. Thus we conclude that it is the preexisting heterogeneous morphology of the microphase-separated block copolymer in the melt that dictates the unusual mode of chain folding observed here. We are currently examining chain folding in semicrystalline diblocks with linear crystallizable blocks to eliminate any possible effect of side chains.

It is also reasonable to enquire into the nature of chain folding for the opposite extreme of sample processing, i.e., the case for which crystallization precedes microphase separation. We have been able to achieve this condition by casting from solution at temperatures well below the melting point. In such samples, however, the lamellar orientations were random, and, therefore, no assignment of a preferred chain direction relative to the lamellar morphology was possible using WAXS pole figures.

Acknowledgment. This research was supported by the Office of Naval Research and by the Bayer Professorship in Chemical Engineering at MIT. Dr. Adel F. Halasa of The Goodyear Tire and Rubber Co. provided several poly(4B2B) precursor diblock copolymer samples that were used in this study. Gilberto Lunardi of PPH Companhia Industrial de Polipropileno, Triunfo, Brazil, performed the dynamic mechanical spectroscopy analysis on the poly(EBEE) samples.

References and Notes

(1) Douzinas, K. C.; Cohen, R. E.; Halasa, A. F. *Macromolecules* **1991**, *24*, 4457.
(2) Whitmore, M. D.; Noolandi, J. *Macromolecules* **1988**, *21*, 1482.
(3) Di Marzio, E. A.; Guttman, C. M.; Hoffman, J. D. *Macromolecules* **1980**, *13*, 1194.
(4) Meier, D. J. *Block and Graft Copolymers*; Burke, J. J., Weiss, V., Eds.; Syracuse University Press: Syracuse, NY, 1973.
(5) Meier, D. J. *Polym. Prepr. (Am. Chem. Soc., Div. Polym. Chem.)* **1974**, *15*, 171.
(6) Helfand, E. *Macromolecules* **1975**, *8*, 552.
(7) Helfand, E.; Wasserman, Z. R. *Macromolecules* **1976**, *9*, 879.
(8) Helfand, E.; Wasserman, Z. R. *Macromolecules* **1978**, *11*, 960.
(9) Leibler, L. *Macromolecules* **1980**, *13*, 1602.
(10) Hashimoto, T. *Macromolecules* **1982**, *15*, 1548.
(11) Hashimoto, T.; Shibayama, M.; Kawai, H. *Macromolecules* **1980**, *13*, 1237.

(12) Bates, F. S.; Berney, C. V.; Cohen, R. E.; Wignall, G. D. *Polymer* **1983**, *24*, 519.
(13) Berney, C. V.; Kofinas, P.; Cohen, R. E. *Polym. Commun.* **1986**, *27*, 330.
(14) Cheng, P.-L.; Berney, C. V.; Cohen, R. E. *Macromolecules* **1988**, *21*, 3442.
(15) Hasegawa, H.; Hasimoto, T.; Kawai, H.; Lodge, T. P.; Amis, E. J.; Glinka, C. J.; Han, C. C. *Macromolecules* **1985**, *18*, 67.
(16) Hadziiouannou, G.; Picot, C.; Skoulios, A.; Ionescu, M.-L.; Mathis, A.; Duplessix, R.; Gallot, Y.; Lingelser, J.-P. *Macromolecules* **1982**, *15*, 263.
(17) Hasegawa, H.; Tanaka, H.; Hashimoto, T.; Han, C. C. *Macromolecules* **1987**, *20*, 2120.
(18) Vilgis, T.; Halperin, A. *Macromolecules* **1991**, *24*, 2090.
(19) Keller, A. *Philos. Magn.* **1957**, *2*, 1171.
(20) Keller, A.; O'Connor, A. *Discuss. Faraday Soc.* **1958**, *25*, 114.
(21) Holland, V. F. *Makromol. Chem.* **1964**, *71*, 204.
(22) Khoury, F.; Passaglia, E. *Treatise on Solid State Chemistry. Vol. 3. Crystalline and Non-Crystalline Solids*; Hannay, N. B., Ed.; Plenum: New York, 1976.
(23) Hirata, E.; Ijitsu, T.; Soen, T.; Hashimoto, T.; Kawai, H. *Polymer* **1975**, *16*, 249.
(24) Cohen, R. E.; Cheng, P. L.; Douzinas, K.; Kofinas, P.; Berney, C. V. *Macromolecules* **1990**, *23*, 324.
(25) Veith, C. A.; Cohen, R. E. *Polymer* **1991**, *32*, 1545.
(26) Halasa, A. F. U.S. Patent 3 872 072.
(27) Bates, F. S.; Cohen, R. E.; Argon, A. S. *Macromolecules* **1983**, *16*, 1108.
(28) Douzinas, K. C. Ph.D. Thesis, Massachusetts Institute of Technology, Cambridge, MA, 1991.
(29) Cullity, B. D. *Elements of X-Ray Diffraction*; Addison-Wesley Publishing Co.: Reading, MA, 1977.
(30) Spruiell, J. E.; Clark, E. S. *Methods of Experimental Physics*; Academic Press: New York, 1980; Vol. 16B, Chapter 6.
(31) Howard, P. R.; Crist, B. *J. Polym. Sci., Part B: Polym. Phys.* **1989**, *27*, 2269.
(32) Han, C. D.; Kim, J.; Kim, J. K. *Macromolecules* **1989**, *22*, 383.
(33) Doi, M.; Edwards, S. F. *J. Chem. Soc., Faraday Trans. 2* **1978**, *74*, 1802, 1818.
(34) Rosedale, J. H.; Bates, F. S. *Macromolecules* **1990**, *23*, 2329.
(35) Desper, C. R.; Stein, R. S. *J. Appl. Phys.* **1966**, *37*, 3990.
(36) Roe, R. J. *J. Appl. Phys.* **1965**, *36*, 2024.
(37) Duncan, K. Pole Figure Applications Software Manual, Rigaku, 1988.
(38) Wunderlich, B. *Macromolecular Physics*; Academic Press: New York, 1976; Vol. 2.